11238–11249 *Nucleic Acids Research, 2019, Vol. 47, No. 21* *Published online 25 September 2019*
doi: 10.1093/nar/gkz814

CDK and Mec1/Tel1-catalyzed phosphorylation of Sae2 regulate different responses to DNA damage

Tai-Yuan Yu[1], Valerie E. Garcia[1] and Lorraine S. Symington[1,2,*]

[1]Department of Microbiology & Immunology, Columbia University Irving Medical Center, New York, NY 10032, USA and [2]Department of Genetics & Development, Columbia University Irving Medical Center, New York, NY 10032, USA

Received February 27, 2019; Revised September 09, 2019; Editorial Decision September 10, 2019; Accepted September 20, 2019

ABSTRACT

Sae2 functions in the DNA damage response by controlling Mre11-Rad50-Xrs2 (MRX)-catalyzed end resection, an essential step for homology-dependent repair of double-strand breaks (DSBs), and by attenuating DNA damage checkpoint signaling. Phosphorylation of Sae2 by cyclin-dependent kinase (CDK1/Cdc28) activates the Mre11 endonuclease, while the physiological role of Sae2 phosphorylation by Mec1 and Tel1 checkpoint kinases is not fully understood. Here, we compare the phenotype of *sae2* mutants lacking the main CDK (*sae2-S267A*) or Mec1 and Tel1 phosphorylation sites (*sae2-5A*) with *sae2Δ* and Mre11 nuclease defective (*mre11-nd*) mutants. The phosphorylation-site mutations confer DNA damage sensitivity, but not to the same extent as *sae2Δ*. The *sae2-S267A* mutation is epistatic to *mre11-nd* for camptothecin (CPT) sensitivity and synergizes with *sgs1Δ*, whereas *sae2-5A* synergizes with *mre11-nd* and exhibits epistasis with *sgs1Δ*. We find that attenuation of checkpoint signaling by Sae2 is mostly independent of Mre11 endonuclease activation but requires Mec1 and Tel1-dependent phosphorylation of Sae2. These results support a model whereby CDK-catalyzed phosphorylation of Sae2 activates resection via Mre11 endonuclease, whereas Sae2 phosphorylation by Mec1 and Tel1 promotes resection by the Dna2-Sgs1 and Exo1 pathways indirectly by dampening the DNA damage response.

INTRODUCTION

Chromosomal double-strand breaks (DSBs) are cytotoxic lesions that must be repaired to maintain genomic integrity. The two main mechanisms used to repair DSBs are non-homologous end joining (NHEJ) and homologous recombination (HR). NHEJ involves the direct ligation of ends and can be mutagenic due to loss or gain of nucleotides at the junction (1). By contrast, HR is considered to be mostly error-free because a homologous duplex is used to template repair. HR begins with 5′-3′ resection of DNA ends to generate long tracts of single-stranded DNA (ssDNA), substrates for the Rad51 recombinase to catalyze homologous pairing and strand invasion (2). Once end resection initiates, cells are committed to HR because long ssDNA overhangs are poor substrates for NHEJ repair. NHEJ predominates in the G1 phase, when cyclin-dependent kinase 1 (CDK1/Cdc28) activity and end resection are low, whereas end resection and HR are activated by CDK1 as cells enter the S and G2 phases of the cell cycle, when a sister chromatid is available to template repair (3). Consequently, regulation of end resection during the cell cycle is a key aspect of repair pathway choice (4).

The *Saccharomyces cerevisiae* MRX complex (MRN in organisms with Nbs1 replacing Xrs2) initiates end resection by endonucleolytic incision of the 5′ strands internal to protein-blocked DNA ends (5–8). CDK-phosphorylated Sae2 (CtIP in mammalian cells) stimulates the Mre11 endonuclease-catalyzed nicking reaction, contributing to cell cycle regulation of end resection (5,8–10). The Mre11 3′-5′ exonuclease degrades from the nick towards the initiating DSB, while Exo1 and Dna2 nuclease activities function redundantly to process the 5′-terminated strands (6,7,11,12). Sgs1 helicase displaces the 5′ strand for Dna2 endonuclease in end resection (12–16). Dna2 nuclear localization is regulated by CDK, which also contributes to cell-cycle regulation of end resection in budding yeast (17). While MRX-Sae2 catalyzed end clipping is essential to remove covalent adducts from DNA ends, Exo1 or Dna2-Sgs1 can directly degrade DSBs produced by endonucleases independently of Mre11 nuclease and Sae2 in budding yeast (18). The Ku heterodimer restricts Exo1 access to DSBs; consequently, resection in *sae2Δ* and *mre11-nd* cells is largely dependent on Dna2-Sgs1 (19–21). Elimination of Ku suppresses the DNA damage sensitivity of *mre11Δ, mre11-nd* and *sae2Δ* cells by allowing Exo1 access to DNA ends (19,20,22–24).

Although *mre11-nd* and *sae2Δ* cells show equivalent defects in removal of covalent adducts, such as Spo11 and DNA hairpins from ends, the *sae2Δ* mutant is more sensitive to DNA damaging agents than *mre11-nd*, and exhibits delayed recovery following activation of the DNA

*To whom correspondence should be addressed. Tel: +1 212 305 4793; Email: lss5@cumc.columbia.edu

damage checkpoint (25,26). Tel1 and Mec1 are the sentinel phosphatidylinositol 3-kinase-related kinases (PIKK) that respond to DSBs in *Saccharomyces cerevisiae* (27). MRX bound to ends recruits and activates Tel1, whereas Mec1-Ddc2 binds to RPA-coated ssDNA generated by end resection. Tel1 and Mec1 redundantly phosphorylate Rad9, which is required for recruitment of the Rad53 effector kinase to damage sites and its subsequent phosphorylation by the PIKK (27). In the absence of Sae2, Mre11 and Tel1 persist at DNA ends and the Tel1 checkpoint is hyperactivated (25,26,28,29). Increased Tel1 activity results in accumulation of Rad9 close to the DSB, which inhibits Dna2-Sgs1 and Exo1-catalyzed end resection, contributing to *sae2Δ* DNA damage sensitivity and end-resection defects (26,30–32). Exo1 is a target for inhibitory phosphorylation by Rad53 (33), while PIKK-catalyzed phosphorylation of Rad9 inhibits resection primarily by the Dna2-Sgs1 mechanism (32,34,35). Even though Mre11 and Tel1 both accumulate at DSBs in the *mre11-nd* mutant, Rad53 is not hyperactivated suggesting that Sae2 dampens the DNA damage checkpoint independent of Mre11 nuclease activation (26).

As described above, CDK-catalyzed phosphorylation of Sae2 Ser-267 plays an important role in regulating MRX activity. In addition, Mec1/ATR and Tel1/ATM phosphorylate Sae2/CtIP on multiple residues in response to DNA damage, but the physiological role of these modifications has not been firmly established (36–38). Substitution of Ser-73, Thr-90, Ser-249, Thr-279 and Ser-289 with alanine (*sae2-5A* mutant) was previously shown to prevent damage-induced phosphorylation of Sae2 and confer a phenotype similar to the *sae2Δ* allele (36,39). Phosphorylation of Sae2 alters the oligomeric state and solubility of Sae2, suggesting that it provides a switch for structural transitions of Sae2 at damaged sites and subsequent turnover of the protein (37,40). ATR and/or ATM phosphorylate the conserved Thr-818 residue of *Xenopus laevis* CtIP (equivalent to Sae2 Thr-279, Thr-859 of human CtIP and Thr-855 of mouse CtIP), and this modification is required for chromatin binding and end resection (38,41,42). Synthetic Sae2 peptides with phosphorylated Thr-90 or Thr-279 residues are able to interact with the FHA domains of Rad53 and Dun1 kinases *in vitro*, and the peptide with phosphorylated Thr-90 additionally interacts with Xrs2 (43). Moreover, the *sae2-T90A, T279A* (*sae2-2A*) mutant is sensitive to MMS and Rad53 remains hyper-phosphorylated following MMS treatment (43). The interaction of phosphorylated Sae2 with the DNA damage effector kinases suggests a role in modulating the DNA damage checkpoint response (26,43). Although interaction between Ctp1, the *Schizosaccharomyces pombe* ortholog of Sae2, and Nbs1 is essential for recruitment of Ctp1 to DSBs and subsequent repair in fission yeast (44), we previously found that end resection in *S. cerevisiae* is independent of Xrs2, but still requires Sae2 (45). Thus, interaction between the Xrs2 FHA domain and Sae2 appears to be dispensable for end resection.

In this study, we investigated how CDK and Mec1 and/or Tel1 (hereafter referred to as PIKK)-catalyzed phosphorylation of Sae2 influences Mre11 endonuclease activity and Dna2-Sgs1 dependent resection. Our studies support the idea that CDK-catalyzed phosphorylation of Sae2 triggers MRX-catalyzed end clipping, which is essential for meiotic recombination, whereas PIKK-dependent phosphorylation promotes DNA damage resistance by down regulating the checkpoint response to facilitate extensive resection.

MATERIALS AND METHODS

Yeast strains and plasmids

The yeast strains used for all experiments except the hairpin-opening assay are derived from W303 corrected for *RAD5* and were constructed via crosses using strains from the lab collection or by one-step gene replacement using PCR-derived DNA fragments (Supplementary Table S1). The *sae2-S267A, sae2-S267E, sae2-2A* and *sae2-5A* derivatives were made by replacement of the *sae2::KIURA3* allele in strain LSY3358 with PCR fragments amplified from plasmids with the corresponding alleles and selecting for 5-FOA resistance. Correct replacement of the *sae2::KlURA3* locus was confirmed by DNA sequencing. The plasmids with each of the MYC tagged *sae2* alleles were described previously (26).

Media and growth conditions

Rich medium (1% yeast extract; 2% peptone; 2% dextrose, YPD), synthetic complete (SC) medium and genetic methods were as described previously (46). CPT or MMS was added to YPD medium at the indicated concentrations. For survival assays, 10-fold serial dilutions of log-phase cultures were spotted on plates with no additive or the indicated amount of drug and incubated for 3 days at 30°C. Diploids homozygous for *sae2* alleles were incubated on solid sporulation medium for 3–4 days and ∼200 cells were scored for the presence of asci. For diploids that sporulated, 50 tetrads were dissected on YPD plates to measure spore viability after 3 days growth. Three independently derived diploids were used for each genotype. Diploids heterozygous for relevant mutations were sporulated and tetrads dissected to assess synthetic genetic interactions. Spores were manipulated on YPD plates and incubated for 3–4 days at 30°C.

In vivo hairpin-opening assay

Strain ALE108 was transformed pRS416-*SAE2*-13MYC, pRS416-*sae2-S267A*-13MYC, pRS416-*sae2-2A*-13MYC or pRS416-*sae2-5A*-13MYC or empty vector to perform the hairpin cleavage assay. The rate of Lys^+ recombinants was derived from the median recombination frequency determined from six different colonies of each strain as described (47). Three trials were performed and the mean recombination rate was calculated.

SSA assay

Cells containing the SSA reporter were cultured in YP containing 2% lactate (YPL) to log phase. Aliquots of cells were collected for isolation of genomic DNA prior to HO induction (0 h), and at one or two hour intervals after addition of galactose to the medium to induce HO expression. Genomic DNA was digested with EcoRV and the resulting blots hybridized with a PCR fragment corresponding

to *LYS2* sequence by Southern blotting. Hybridizing fragments were quantified and the percent cut fragment, donor fragment and SSA product determined by the ratio of each fragment to total hybridizing DNA. SSA efficiency was also measured by qPCR. We designed primer pairs to amplify sequences 3 kb downstream of the HO cut site (HOcs) between the two *lys2* fragments (3K_DS), and 3.2 kb upstream of the HOcs (3.2K_US). The Ct values for each primer pair were normalized to *ADH1*, and the SSA product was calculated using the ratio of 3K_DS/3.2K_US.

Rad53 Western blot

Yeast cells were grown to 10^7 cells/ml in YPD, then 0.015% MMS or 50 μg/ml zeocin was added for 1 h. Cells were released into fresh YPD medium and collected at the indicated time points for TCA precipitation. Cells were resuspended in 0.2 ml 20% TCA and then mechanically disrupted for 5 min using glass beads. Beads were washed twice with 0.2 ml 5% TCA each and pellets collected by centrifugation. The pellet was resuspended in 0.15 ml SDS-PAGE sample buffer and proteins separated by SDS-PAGE. Anti-Rad53 antibodies were used for immunoblots.

Chromatin immunoprecipitation (ChIP) assays

Yeast cells were cultured in YP containing 2% lactate (YPL) to log phase and arrested at G2/M phase by adding nocodazole (15 μg/ml) to the medium. For Sae2 and Rad9 ChIP analyses, plasmids containing MYC-tagged *sae2* alleles were expressed in a *sae2Δ* strain and cultured in synthetic medium with raffinose as a carbon source. For ChIP experiments, cells were collected prior to, and 3 h after adding galactose to 2% for HO endonuclease induction. After formaldehyde cross-linking and chromatin isolation, Mre11, HA-Tel1, Rad9-HA or Sae2-MYC were immunoprecipitated as described previously using Mre11 polyclonal antibodies from rabbit serum, anti-HA antibodies (16B12, BioLegend) or anti-MYC antibodies (9E10, Santa Cruz) respectively (48,49). Quantitative PCR was carried out using SYBR green real-time PCR mix (Biorad) and primers complementary to DNA sequences located 0.2 kb from the HO-cut site at the *MAT* locus. Reads were normalized to DNA sequences located 66 kb from the HO site.

RESULTS

Mutation of Sae2 phosphorylation sites confers modest DNA damage sensitivity

To evaluate the roles of cell cycle and DNA damage-induced phosphorylation on Sae2 function, we generated Sae2 variants with substitution mutations at sites previously identified as targets for CDK or PIKK-dependent phosphorylation (Figure 1A) (9,36,37,40). Initially, *sae2-S267A, sae2-2A* (T90A, T279A) and *sae2-5A* (S73A, T90A, S249A, T279A, S289A) alleles were generated in a low-copy number plasmid and were fused to a MYC epitope to evaluate steady-state protein levels. All of the Sae2 mutants tested are expressed at similar levels to wild-type Sae2 and do not alter the steady state level of Mre11 (Figure 1B). These alleles (without the MYC tag) were then generated at the endogenous *SAE2* locus for subsequent genetic analysis. We chose to characterize the *sae2-2A* mutation in addition to *sae2-5A* to determine whether Thr-90 and Thr-279 are the main residues contributing to the *sae2-5A* phenotype. Our previous studies have shown that the *sae2Δ* mutant exhibits greater sensitivity to camptothecin (CPT) and methyl methane sulfonate (MMS) than cells lacking Mre11 nuclease (*mre11-H125N* and *mre11-D56N* mutants) (26,50). CPT traps the Top1 covalent intermediate resulting in replication-dependent DSBs, whereas the alkylated bases generated by MMS cause replication stress. If the primary function of CDK-catalyzed phosphorylation of Sae2 Ser-267 is to stimulate Mre11 endonuclease activity, then we anticipated the *sae2-S267A* and *mre11-H125N* mutants to show equivalent DNA damage sensitivity. We find the *sae2-S267A* mutant to be more resistant to CPT and MMS than the *sae2Δ* mutant, and slightly more resistant than the *mre11-H125N* mutant (Figure 1C). The *sae2-S267E* mutant has similar resistance to wild type (WT). The *sae2-S267A* mutant was originally reported to confer a phenotype indistinguishable from the *sae2Δ* mutant (9); however, a more recent study showed only modest DNA damage sensitivity of *sae2-S267A* cells (37), in agreement with our data.

Note that in accord with our previous studies, the *mre11-D56N* mutant exhibits slightly higher CPT and MMS resistance than *mre11-H125N*, even though both lack nuclease activity *in vitro* and have equivalent defects in removal of covalent adducts from ends (Figure 1C) (11,47,48,51). Asp-56 coordinates both Mn^{2+} ions within the Mre11 nuclease catalytic site, whereas His-125 is proposed to stabilize the transition intermediate by donating a proton to the leaving 3′-OH after Mn^{2+}-mediated hydroxyl attack of the sugar-3′-*O*-phosphate bond of the substrate DNA (52). Thus, His-125 acts at a step after metal binding. It is possible that metal binding without subsequent catalysis causes a subtle conformational change to the MRX complex that alters the ability of the alternate resection mechanisms to access DNA ends. It is interesting to note that a gain of function *mre11* mutation has been reported that promotes access of Exo1 to DNA ends suggesting that the conformation and/or turnover of the MRX complex at ends can influence the extensive resection mechanisms (53).

The *sae2-5A* mutant exhibits greater sensitivity to DNA damage than *sae2-S267A* and *mre11-H125N* mutants (Figure 1C). Previous studies showed that the *sae2-T90A* and *sae2-T279A* single mutations confer no obvious DNA damage sensitivity, and the *sae2-2A* mutant is more sensitive to CPT and MMS than WT cells (43). We find the *sae2-2A* mutant to be slightly more sensitive to DNA damage than *sae2-S267A*, similar to the *sae2-5A* mutant.

The *sae2-S267A* mutation is epistatic to *mre11-H125N* and synergistic with *sgs1Δ*

The *mre11-H125N sae2-S267A* double mutant exhibits similar CPT resistance to the *sae2-S267A* single mutant, whereas the *mre11-H125N sae2-2A* and *mre11-H125N sae2-5A* mutants are more sensitive to CPT than the single mutants (Figure 1C, D). The slight suppression of the *mre11-H125N* phenotype by *sae2-S267A* is reminiscent of the suppression of *mre11-H125N* by the *D56N* mutation

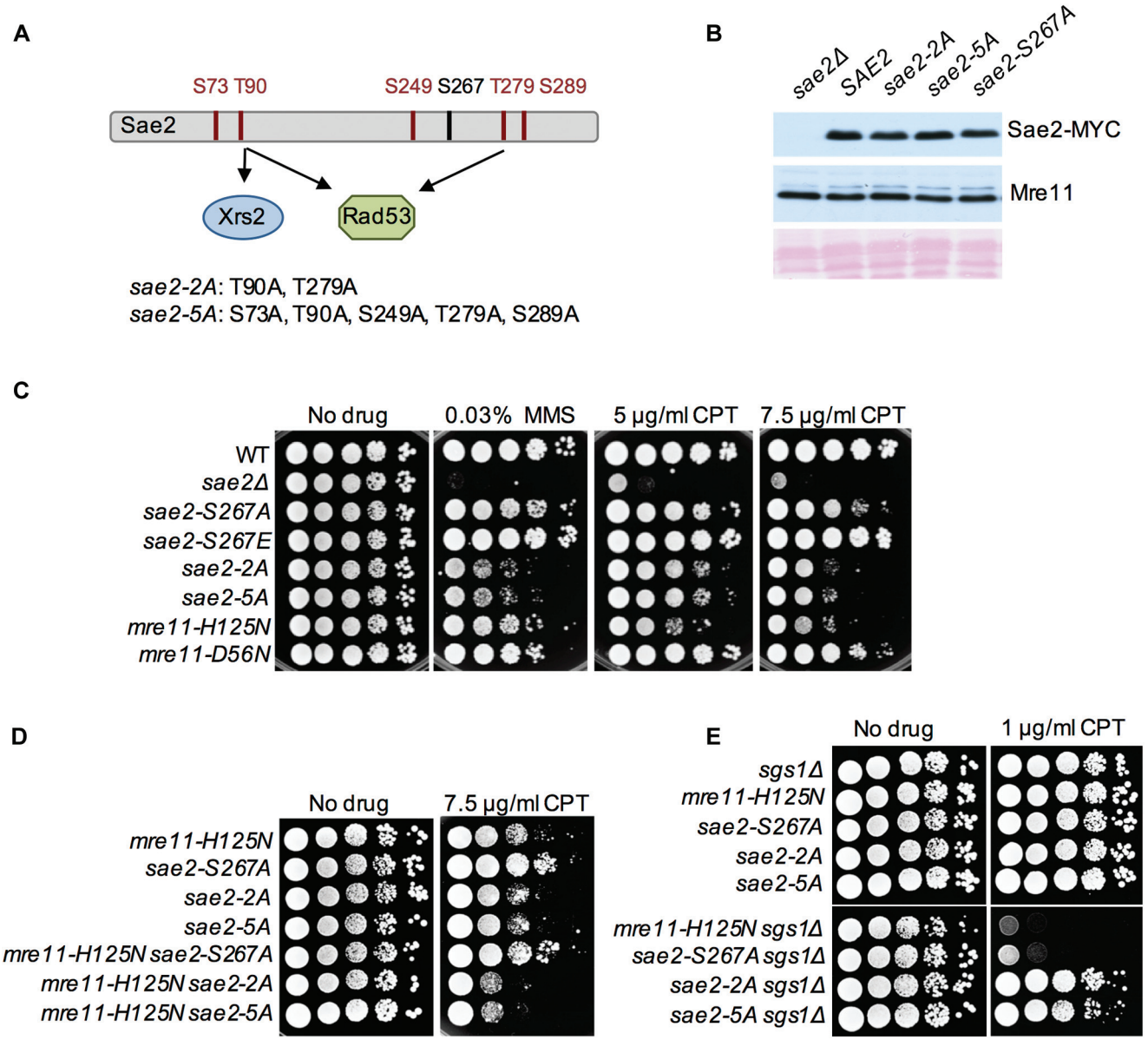

Figure 1. CDK-dependent phosphorylation of Sae2 is epistatic to Mre11 endonuclease activity. (**A**) Location of the phosphorylated Sae2 residues tested in this study. The main PIKK sites are marked in red and the CDK site tested is marked in black. (**B**) Western blot showing steady state levels of Sae2-MYC and Mre11 in the indicated strains. The lower panel shows Ponceau red stain of the membrane used for Western blot. (**C**–**E**) Ten-fold serial dilutions of the indicated strains spotted on plates without drug, or plates containing camptothecin (CPT) or methyl methanesulfonate (MMS) at the indicated concentrations. At least three independent trials (using different isolates of the same genotype) of spot assays were carried out and representative plates are shown. WT refers to wild type and Δ indicates null allele.

that we previously reported (48). Since phosphorylated Sae2 has been shown to interact with Rad50 and the Rad50 ATPase is essential for Mre11 dsDNA endonuclease activation (5,40), we suggest that this interaction is essential to initiate catalysis at a step before the transition state stabilized by His-125 explaining the suppression of *mre11-H125N* by either *D56N* or *sae2-S267A*. To test this idea, we compared the CPT sensitivity of the *sae2-S267A* allele in combination with *mre11-D56N*. As noted above, the *mre11-D56N* mutant is slightly more resistant to CPT than *mre11-H125N*, like *sae2-S267A,* and the *mre11-D56N sae2-S267A* double mutant is indistinguishable from the single mutants (Supplementary Figure S1A). Similar to *mre11-H125N, mre11-D56N* synergizes with *sae2-5A*. These data are consistent with CDK-mediated phosphorylation of Sae2 activating Mre11 endonuclease, and suggest that PIKK-dependent phosphorylation is required for a different function of Sae2 that confers DNA damage resistance.

Previous studies have shown that Mre11 nuclease deficiency causes synergistic DNA damage sensitivity and end resection defects in the *sgs1Δ* background, and the *sae2Δ sgs1Δ* double mutant is inviable (19–21). These data suggest that Dna2-Sgs1 dependent resection can substitute for MRX-Sae2-catalyzed end clipping to initiate end resection.

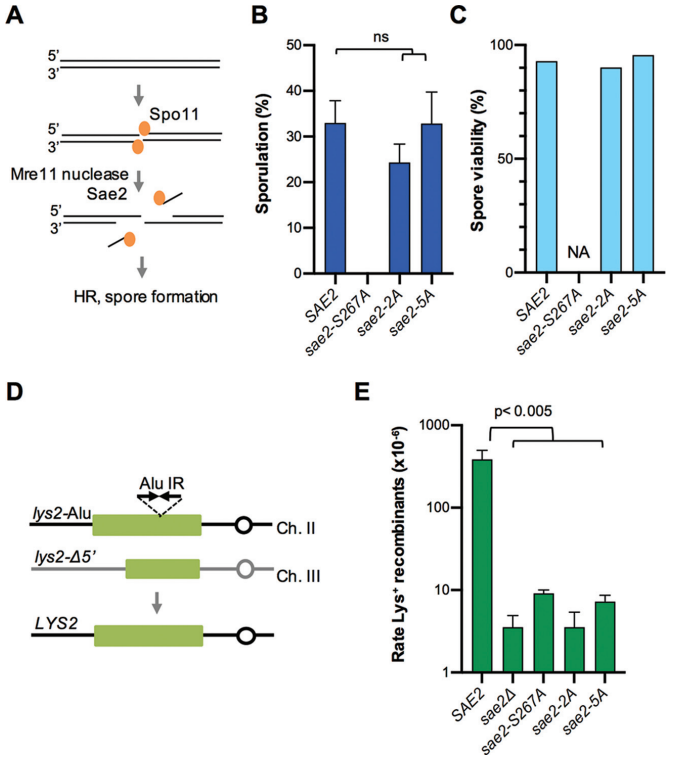

Figure 2. PIKK-dependent phosphorylation of Sae2 is dispensable for sporulation and production of viable spores. (**A**) Schematic of meiotic DSB formation and release of Spo11-oligonucleotides. (**B**) Percent sporulation of the indicated strains. Error bars indicate standard deviation from three independent trials. (**C**) Viability of dissected tetrads. At least 50 tetrads were dissected from each strain. No tetrads were recovered from the *sae2-S267A* strain; therefore, viability is not applicable (NA). (**D**) Cartoon representation of the *lys2-AluIR* ectopic recombination assay. (**E**) Recombination frequencies of strains with the *lys2-AluIR* and *lys2-Δ5′* ectopic recombination reporter system. The rate of Lys^+ recombinants was derived from the median recombination frequency determined from six different isolates of each strain. Error bars indicate s.d. ($n = 3$).

By contrast to *sae2Δ*, the *sae2-S267A, sae2-2A* and *sae2-5A* alleles are viable with *sgs1Δ* (Figure 1E). Like *mre11-H125N*, the *sae2-S267A* mutation synergizes with *sgs1Δ* for CPT sensitivity, consistent with a defect in activation of Mre11 endonuclease. The *sae2-2A sgs1Δ* and *sae2-5A sgs1Δ* double mutants exhibit similar CPT sensitivity to the *sgs1Δ* single mutant at low CPT concentration (Figure 1E); however, at a higher CPT concentration the double mutants are more sensitive than the single mutants (Supplementary Figure S1B). Because *sae2-2A* and *sae2-5A* show epistasis with *sgs1Δ* at a CPT concentration that results in lethality of *mre11-H125N sgs1Δ* cells, we suggest that Mre11 endonuclease is active in *sae2-2A* and *sae2-5A* cells. The CPT sensitivity of *sae2-2A sgs1Δ* and *sae2-5A sgs1Δ* cells at higher CPT concentrations indicates that PIKK-catalyzed phosphorylation of Sae2 is important for Exo1 activity. A previous study identified Exo1 as a substrate for Rad53 and we found that an *exo1* variant lacking the major Rad53 phosphorylation sites suppresses the DNA damage sensitivity of *sae2Δ* cells, consistent with negative regulation of Exo1 by the DNA damage checkpoint (26,33). We also compared the CPT sensitivity of *sgs1Δ mre11-D56N, sgs1Δ mre11-H125N* and *sgs1Δ sae2-S267A* cells with the *sgs1Δ* mutant. A strong synergism was found for all double mutants with *mre11-D56N sgs1Δ* and *sae2-S267A sgs1Δ* exhibiting slightly better growth and CPT resistance than *mre11-H125N sgs1Δ* (Supplementary Figure S1C). All studies hereafter, use *mre11-H125N* as a representative *mre11-nd* mutation.

Resection initiation is impaired in *sae2-S267A* cells

To assess the role of Sae2 phosphorylation in resection initiation via Mre11, the phosphorylation site mutants were tested for defects in meiosis and hairpin resolution. Spo11, a topoisomerase-like protein, initiates meiotic recombination by cleaving both DNA strands at recombination hotspots and remains covalently bound to the 5′ ends(Figure 2A) (54). Removal of Spo11 attached to a short oligonucleotide is essential for subsequent steps of HR and spore formation, and is catalyzed by Mre11 endonuclease and Sae2 (11,55). Previous studies have shown that *mre11-nd, sae2Δ, sae2-5A* and *sae2-S267A* diploids fail to sporulate in the SK1 strain background, consistent with impaired removal of Spo11 (9,36,56,57). As expected, we obtain no spores from the *sae2-S267A* diploid; however, the percent sporulation of *sae2-2A* cells is not significantly different to WT ($P = 0.08$), and viability of dissected ascospores is also normal (Figure 2B, C). Thus, PIKK-dependent phosphorylation of Thr-90 and Thr-279 is not required for release of Spo11 oligonucleotides. Surprisingly, we find sporulation and spore viability of the *sae2-5A* mutant are also the same as WT. Because this result was unexpected we sequenced the *SAE2* locus from all four viable spores derived from a single tetrad and confirmed the presence of the *sae2-5A* allele in each spore clone. We do not know the reason for the discrepancy between our data and the previous report regarding sporulation of the *sae2-5A* mutant (36,39). Our studies are performed in the W303 background, whereas the previous studies used the SK1 yeast strain background.

Hairpin cleavage was assessed using a previously described genetic assay (Figure 2D). Lobachev et al. reported that inverted Alu repeats stimulate recombination ∼1000-fold when compared with Alu repeats inserted as a direct repeat, and this increase is dependent on Mre11 endonuclease and Sae2 (47). The inverted Alu repeats inserted at the *lys2* locus are thought to extrude to form a hairpin during DNA replication, which is cleaved by MRX-Sae2 and subsequently repaired by HR using a truncated *lys2* donor (58). An alternative model posits formation of a cruciform structure at the inverted Alus that is resolved by a Holliday junction endonuclease; the resulting hairpin-capped ends would need to be cleaved by MRX/Sae2 for homology-directed repair (47). We found a >40-fold reduction in the rate of Lys^+ recombinants in all of the *sae2* phosphorylation-site mutants relative to the *SAE2* strain ($P<0.005$), suggesting defects in hairpin cleavage and/or the subsequent processing steps to yield Lys^+ recombinants (Figure 2E).

PIKK-dependent phosphorylation of Sae2 promotes extensive resection

We assessed end resection at an HO endonuclease-induced DSB using a single-strand annealing (SSA) assay. The re-

porter is comprised of two overlapping fragments of the *lys2* gene with 2.2 kb homology, separated by 20 kb on chromosome V (Figure 3A) (26). An HO endonuclease cut site is located at the junction of one *lys2* repeat and the intervening sequence. Additionally, the strains contain a galactose-inducible *HO* gene and a *rad51Δ* mutation to prevent repair by break-induced replication. Following DSB induction, the single-stranded regions of *lys2* exposed by end resection anneal to restore *LYS2*, accompanied by deletion of one of the repeats and intervening sequence. Because successful SSA requires degradation of 20 kb it is a sensitive assay for defects in extensive end resection by Dna2-Sgs1 and Exo1 (12,14,59). SSA was monitored by blot hybridization of EcoRV digested genomic DNA isolated at different times after HO induction, and by a qPCR assay that measures loss of sequence between the repeats.

We previously showed a delay in end resection, as visualized by persistence of the 3.2 kb cut fragment and delayed disappearance of the downstream 2.6 kb fragment, coupled to a lag in deletion product formation in the *sae2Δ* mutant as compared to WT (26). The *sae2-S267A* and *sae2-2A* mutants exhibit a subtle delay in SSA product formation, and the *sae2-5A* phenotype is intermediate between *sae2-2A* and *sae2Δ* (Figure 3B, C, Supplementary Figure S2). If the DNA damage sensitivity of the strains reflects defective end resection then we anticipated the *mre11-nd sae2-S267A* mutant to behave similarly to the single mutants, and for a more severe SSA defect for the *mre11-nd sae2-5A* double mutant. Consistently, the *sae2-5A* mutation synergizes with *mre11-nd*, while *sae2-S267A* is epistatic to *mre11-nd* by the SSA assay (Figure 3D). These data confirm that CDK-dependent phosphorylation of Sae2 activates Mre11 endonuclease. Since the *sae2-5A* mutant is proficient for sporulation, indicating normal Mre11 endonuclease activation, but is defective for SSA, we conclude that PIKK-dependent phosphorylation of Sae2 is required for optimal resection by Exo1 and/or Dna2-Sgs1.

PIKK-catalyzed phosphorylation of Sae2 alters the checkpoint response

Sae2-deficient cells show hyper activation of Rad53/Chk2 kinase in response to DNA damage and slower recovery from checkpoint-mediated cell-cycle arrest; *sae2-5A* and *sae2-2A* mutants share this phenotype (25,43). Hyperactivation of the DNA damage checkpoint results in increased Rad9 binding near the initiating DSB, reducing extensive end resection (30–32,60). Because end resection in yeast is fast, Rad53 phosphorylation in response to DSBs is mainly through the Mec1 branch of the pathway. To specifically monitor Tel1-dependent checkpoint activation, we compared Rad53 phosphorylation in *mec1Δ sml1Δ* (*sml1Δ* is required to suppress lethality of *mec1Δ*) derivatives of *sae2* and *mre11-nd* mutants. Cells were treated with MMS for one hour, and then released into MMS-free medium and different time points were taken to assess Rad53 phosphorylation by Western blot. We find the *sae2-S267A* mutant to be similar to *mre11-nd* with slightly increased phosphorylation of Rad53 compared with *SAE2* or *MRE11* cells, but with lower Rad53 activation than observed in *sae2-2A* and *sae2-5A* cells (Figure 4A). Combining *mre11-nd* with *sae2-S267A, sae2-2A* or *sae2-5A* does not alter the checkpoint response relative to the single mutants, suggesting that PIKK-phosphorylated Sae2 has a role in suppressing Tel1 activation that is independent of Mre11 nuclease activity. A similar response was observed when cells were treated with zeocin to directly induce DSBs (Supplementary Figure S3A). We also monitored Rad53 activation and recovery in *MEC1* cells. Again, *sae2-S267A* shows slightly increased Rad53 phosphorylation as compared to WT and delayed recovery from checkpoint activation, and the *mre11-nd sae2-S267A* double mutant is similar to the single mutants (Supplementary Figure S3B). By contrast, *sae2-2A* and *sae2-2A mre11-nd* mutants show more persistent Rad53 phosphorylation.

During the course of strain construction by genetic cross we found that the *sae2-2A* mutation suppresses lethality of *mec1Δ SML1* cells (Figure 4B), a phenotype we recently reported for *sae2Δ* and *sae2-5A* mutations (26). By contrast, no colonies or very small colonies were obtained for *mec1Δ sae2-S267A* and *mec1Δ mre11-nd sae2-S267A* mutants by genetic cross. We suggest that suppression of *mec1Δ* lethality by *sae2-2A, sae2-5A* and *sae2Δ* is due to the role of Tel1-dependent phosphorylation of Sae2 in negatively regulating Rad9 accumulation at damaged sites (26,43).

Rad9 accumulates at DSBs in the *sae2-2A* and *sae2-5A* mutants

Rad53 activation by Tel1 requires MRX and Rad9 binding in the vicinity of DSBs. Previous studies have shown that Mre11, Tel1 and Rad9 accumulate to higher levels adjacent to an HO-induced DSB in *sae2Δ* cells as compared to WT (26,30–32). Even though Mre11 and Tel1 are retained at DSBs for longer in *mre11-nd* cells than observed for WT, Rad9 fails to accumulate explaining the weaker Rad53 activation and more proficient end resection in *mre11-nd* than observed in *sae2Δ* cells (26). We measured Mre11, Tel1 and Rad9 association with sequences close to the HO endonuclease cut site at the *MAT* locus on chromosome III by chromatin immunoprecipitation (ChIP) before and after HO expression in the *sae2* derivatives (Figure 4C and Supplementary Figure S4). We find increased retention of Mre11 and Tel1 at DSBs in the *sae2-S267A* mutant, consistent with a resection initiation defect, whereas Mre11 and Tel1 binding are not significantly increased in *sae2-2A* and *sae2-5A* mutants (Figure 4D, E). However, Rad9 retention close to the DSB is slightly higher in *sae2-2A* and *sae2-5A* mutants than WT (Figure 4F). These findings are consistent with the increased Rad53 activation observed in *sae2-2A* and *sae2-5A* mutants and indicate that the checkpoint dampening function of Sae2 is not driven solely by MRX and Tel1 retention at DSBs. Although Rad9 binding close to the DSB appears higher in the *sae2-S267A* mutant than in WT, the difference is not statistically significant (Figure 4F).

PIKK-dependent phosphorylation of Sae2 is required for stable chromatin binding

The *X. laevis* CtIP-T818A protein is defective for chromatin binding, suggesting that ATR or ATM-catalyzed phosphorylation of CtIP is required for association with damaged

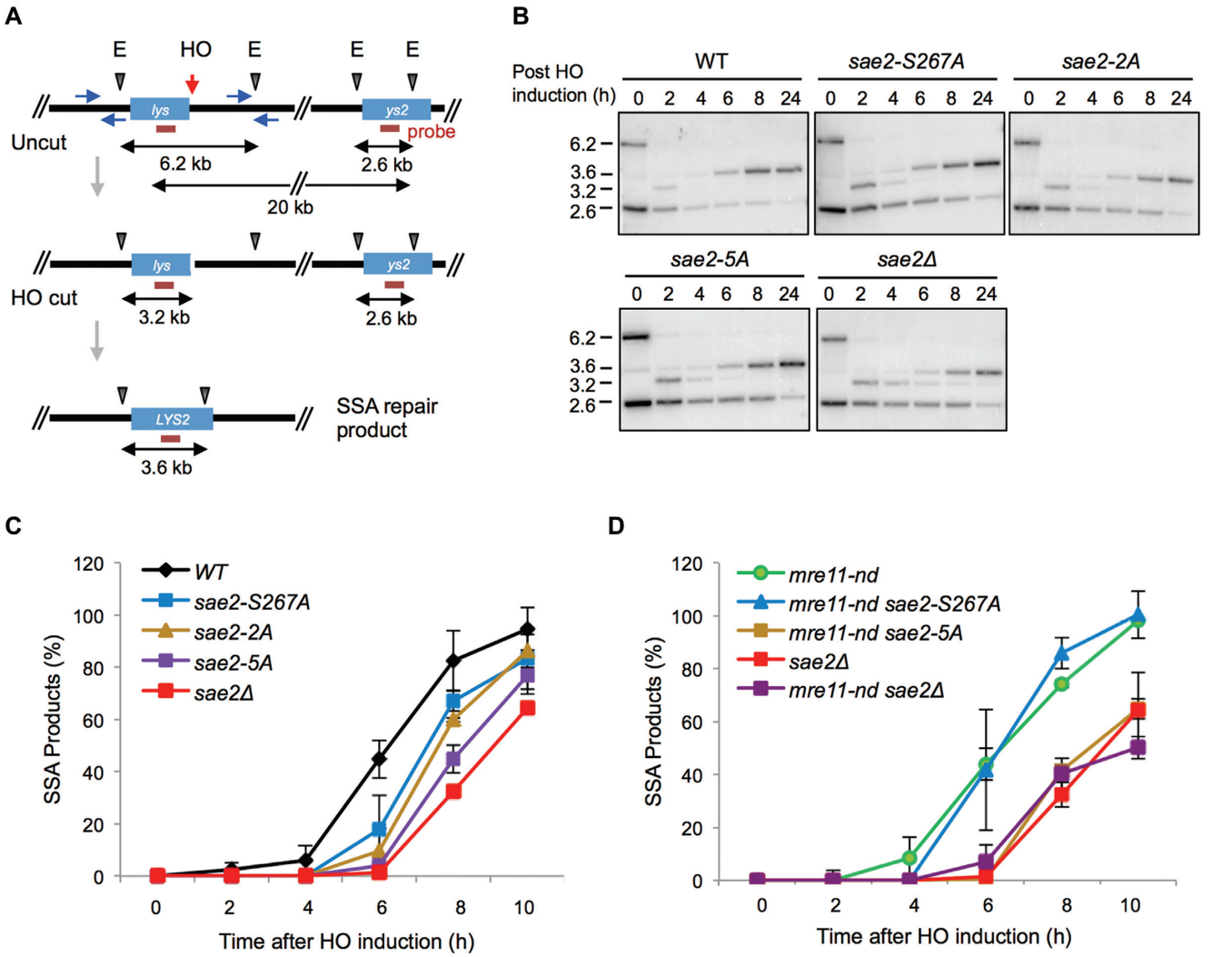

Figure 3. PIKK-dependent phosphorylation of Sae2 is required for extensive resection. (**A**) Schematic of the SSA assay (see text for details) showing the location of EcoRV (E) sites used to monitor SSA product formation by genomic DNA digest and Southern blot. The horizontal red line shows the location of the probe used for Southern blot hybridization. The horizontal blue arrows indicate the primer pairs used for qPCR to detect SSA products. (**B**) Representative Southern blots of the indicated strains pre HO and at different times (h) after HO induction. (**C**, **D**) Quantification of SSA by a qPCR assay measuring loss of sequence between the *lys2* fragments. Error bars indicate SD from three independent trials of the indicated strains.

sites (38,41). To determine whether this function is conserved, we measured Sae2 binding 0.2 kb from the HO cut site by ChIP (Figure 4G). The sae2-S267A mutant protein is retained at a higher level than Sae2, whereas sae2-2A and sae2-5A are retained at much lower levels than Sae2, but at a significantly higher level than the no tag control strain ($P<0.05$). We combined the *sae2-2A* and *sae2-5A* mutations with *mre11-nd* to determine whether the failure to maintain the mutant proteins is simply due to normal resection initiation, but even in the *mre11-nd* background sae2-2A and sae2-5A are not enriched at DSBs (Figure 4H). Mre11 endonuclease activation appears to be normal in *sae2-2A* and *sae2-5A* cells indicating that stable binding to chromatin is not required for this function of Sae2. The failure to detect stable association of sae2-2A and sae2-5A to chromatin is consistent with data from *X. laevis* egg extracts showing that phosphorylation of CtIP T818 is required for chromatin binding (41). Furthermore, our data suggest that the previously reported resection defect caused by the *X. laevis* CtIP-T818A (T855A/T859A in mouse/human) mutant is due to impaired resection by Exo1 or Dna2 rather than failure to activate the Mre11 endonuclease (38,41,42).

Structural and biochemical studies have shown that phosphorylated Ctp1 and CtIP interact with the FHA domain of Nbs1, and the Nbs1 FHA domain is required for recruitment of Ctp1 to DSBs in *S. pombe* (44,61,62). In agreement with these findings, a synthetic Sae2 peptide with phosphorylated Thr-90 is able to interact with the FHA domain of Xrs2 (43). To explore the functional significance of the Sae2–Xrs2 interaction, we compared the DNA damage sensitivity of the *xrs2-S47A, H50A* (*xrs2-SH*) mutant with *mre11-nd* and *sae2-5A*. The equivalent residues to S47 and H50 in other FHA domain containing proteins are required for interaction with phosphorylated threonine residues (63), and the *xrs2-SH* mutant was previously shown to be defective for NHEJ (45,64,65). By con-

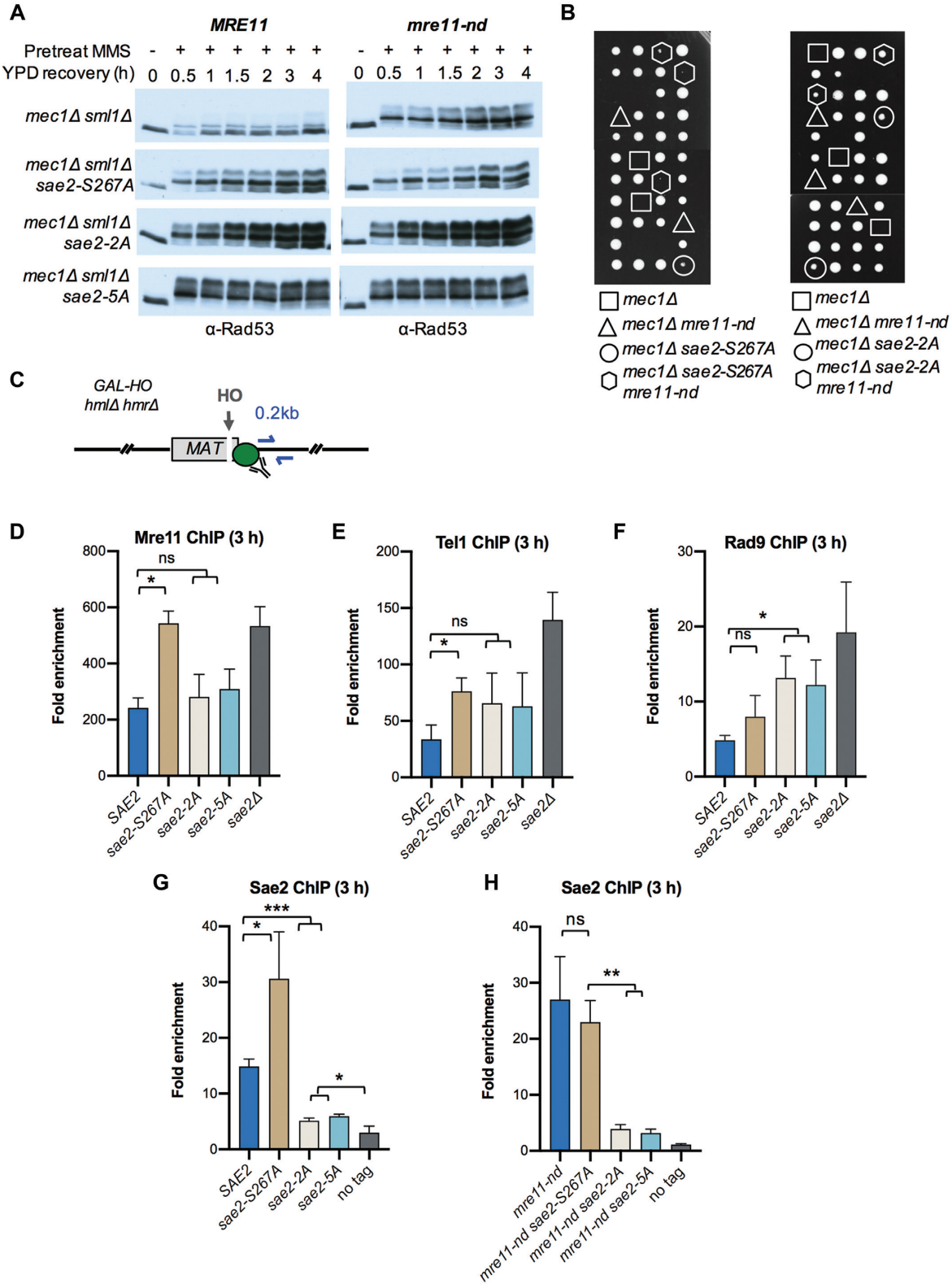

Figure 4. PIKK-dependent phosphorylation of Sae2 attenuates Rad53 activation. (**A**) Log phase cells from the indicated strains were treated with 0.015% MMS for 1 h, released into fresh YPD and protein samples from different time points before (t = 0h) and after drug treatment ($t = 0.5$–4 h) were analyzed using anti-Rad53 antibodies. (**B**) *SAE2/sae2-2A* or *SAE2/sae2-S267A MRE11/mre11-nd mec1Δ/MEC1 sml1Δ/SML1* heterozygous diploids were sporulated and tetrads were dissected on YPD plates. (**C**) Schematic showing location of the primers used for qPCR relative to the HO cut site. All strains for ChIP-qPCR contain *GAL-HO* and deletions of *HML* and *HMR* to prevent HR. The relative fold enrichment of Mre11 (**D**), HA-Tel1 (**E**) and Rad9-HA (**F**) or Sae2-MYC (**G**, **H**) at 0.2 kb from the HO site was evaluated by qPCR after ChIP with anti-Mre11, anti-HA or anti-MYC antibodies, respectively. The 0 h time point is shown in Supplementary Figure S4. Note that only the 3 h time point is shown for the Sae2 ChIP with the no tag control strain. Error bars indicate SD from three independent trials. *P* values of <0.05 are indicated by * <0.01 by ** and <0.001 by ***.

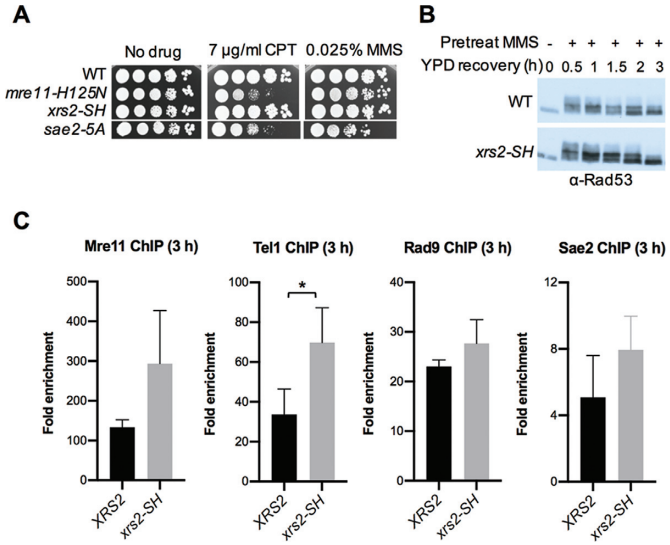

Figure 5. Sae2 binds to DSBs independently of the Xrs2 FHA domain. (**A**) Ten-fold serial dilutions of the indicated strains spotted on plates without drug, or plates containing CPT or MMS at the indicated concentrations. Three independent trials of spot assays were carried out and representative plates are shown. (**B**) Log phase cells from the indicated strains were treated with 0.015% MMS for 1 h, released into fresh YPD and protein samples from different time points before ($t = 0$ h) and after drug treatment ($t =$ 0.5–4 h) were analyzed using anti-Rad53 antibodies. (**C**) The relative fold enrichment of Mre11, HA-Tel1, Rad9-HA or Sae2-MYC at 0.2 kb from the HO site was evaluated by qPCR after ChIP with anti-Mre11, anti-HA or anti-MYC antibodies, respectively. Error bars indicate SD from three independent trials.

trast to *sae2-5A*, the *xrs2-SH* mutant exhibits no obvious DNA damage sensitivity (Figure 5A). Furthermore, Rad53 is not hyper-phosphorylated in *xrs2-SH* cells (Figure 5B). Although Mre11, Tel1 and Rad9 binding adjacent to an HO-induced DSB is slightly higher in *xrs2-SH* cells, the difference is only significant for Tel1. Surprisingly, we find no difference in the level of Sae2 at DSBs between WT and the *xrs2-SH* mutant (Figure 5C). These data are consistent with previous studies in budding yeast showing that Sae2 interacts with Mre11 and Rad50 (5,40), and the finding of Sae2-dependent resection in cells lacking Xrs2 (45).

DISCUSSION

The goal of this study was to elucidate the physiological roles of CDK and PIKK-dependent phosphorylation of the conserved Sae2/CtIP protein. With respect to DNA damage sensitivity, Mre11 and Sae2 retention at an endonuclease-induced DSB, checkpoint attenuation and meiotic recombination, the *sae2-S267A* mutant behaves similarly to cells lacking Mre11 nuclease, consistent with *in vitro* studies showing that CDK-catalyzed phosphorylation of Sae2 Ser-267 activates the Mre11 nuclease to cleave protein-blocked ends (Figure 6 and Supplementary Figure S5) (5–7,40). By contrast, we find that PIKK-catalyzed phosphorylation promotes DNA damage resistance by attenuating DNA damage signaling. The synergism between *sae2-2A* or *sae2-5A* with *mre11-nd* is most consistent with PIKK-dependent phosphorylation of Sae2 acting independently of Mre11 nuclease activation. Furthermore, the synergistic interaction between *sgs1Δ* and *mre11-D56N, mre11-H125N* or *sae2-S267A* and epistatic interaction between *sgs1Δ* and *sae2-2A* or *sae2-5A* mutations is most consistent with distinct functions of Sae2: CDK-mediated activation of Mre11 endonuclease and PIKK-mediated indirect activation of Dna2-Sgs1 and Exo1-catalyzed end resection via checkpoint attenuation. The phenotypic similarity between *sae2-2A* and *sae2-5A* mutants indicates that phosphorylation of Thr-90 and Thr-279 is mainly responsible for the checkpoint attenuation function of Sae2. Because Mre11 and Tel1 do not accumulate to high levels in the *sae2-2A* and *sae2-5A* mutants, we suggest that checkpoint hyperactivation in the *sae2Δ* mutant is not driven solely by delayed turnover of Mre11 at DSBs. A previous study reported that phosphorylated Thr-90 and Thr-279 direct interaction with the FHA domains of Dun1, Rad53 and Xrs2 (43). We suggest that the Sae2-Xrs2 interaction is more important for regulating the checkpoint response than for resection initiation, and that the previously reported Sae2-Rad53 interaction may attenuate Rad53 activation (26,42).

Our studies indicate that stable Sae2 recruitment to chromatin requires PIKK-dependent phosphorylation but is independent of the Xrs2 FHA domain. We propose that Sae2 activation of Mre11 endonuclease requires only a transient interaction between the proteins, whereas stable retention of Sae2 is important for checkpoint attenuation. Retention of sae2-2A and sae2-5A at DSBs is above background and the residual binding could occur via Mre11 or Rad50 in-

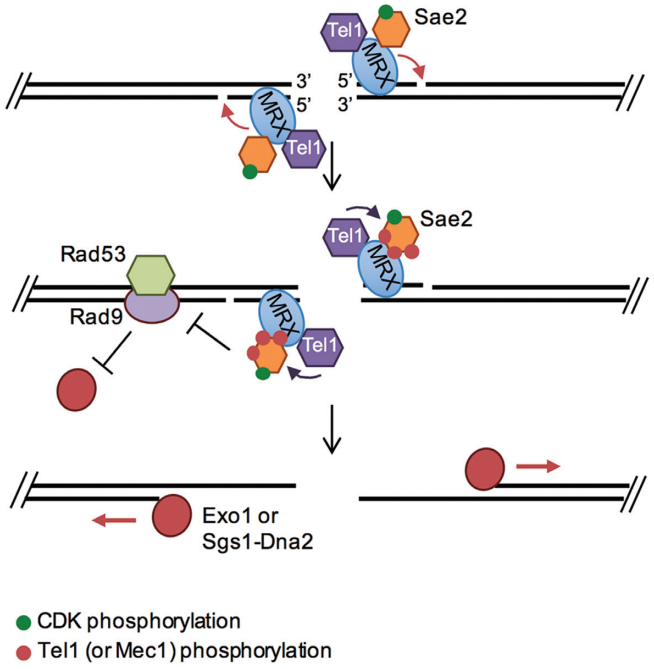

Figure 6. Model for the role of Sae2 phosphorylation by CDK and PIKK kinases. In the S-G2 phase of the cell cycle, CDK phosphorylates Sae2 on Ser-267, activating the Mre11 endonuclease. If resection initiation is delayed, for example by the *mre11-nd* mutation, Tel1 phosphorylates Sae2, which then dampens Rad53 activation by inhibiting Rad9 binding to chromatin and to Rad53 (26). The checkpoint attenuation function of Sae2 allows more efficient resection by Exo1 or Sgs1-Dna2 by relieving the inhibition imposed by Rad9 and Rad53.

teraction. Alternatively, since dephosphorylated Sae2 exhibits higher affinity for dsDNA than phosphorylated Sae2 it raises the possibility of direct interaction between sae2-2A and sae2-5A with DNA at DSBs independent of MRX (40).

Previous studies have shown that Spo11 removal from 5′ ends at meiotic DSBs by Mre11 endonuclease and Sae2 is essential for meiosis; failure to remove Spo11 results in unprocessed DSBs, inability to load Dmc1 and Rad51 recombinases, meiotic arrest and failure to produce viable haploid spores (54). In contrast to an endonuclease-induced DSB, where Sgs1-Dna2 or Exo1 can substitute for loss of MRX clipping, Sgs1-Dna2 and Exo1 are unable to process Spo11-bound DSBs. Cells can only complete sporulation and generate viable spores if Spo11 has been removed from DSB ends by MRX; thus, proficiency for sporulation is a robust readout for Mre11 nuclease activity. We show that the *sae2-S267A* homozygous diploid, like *mre11-H125N* and *sae2Δ* diploids, is unable to sporulate, whereas *sae2-2A* and *sae2-5A* homozygous diploids are sporulation proficient and yield viable spores indicating that Spo11 must have been removed from ends. A recent study showed that a sae2 variant with S73A, T90A, T249A and T279A mutations and the sae2-S289A mutant are both proficient for activation of Mre11 endonuclease *in vitro* (40), consistent with our finding that *sae2-2A* and *sae2-5A* diploids are sporulation proficient. Although the PIKK sites mutated in the *sae2-5A* allele eliminate most damage-induced phosphorylation of Sae2 (36), it remains possible that some of the other phosphorylation sites detected by mass spectrometry analysis contribute to Sae2 function in meiosis and in the DNA damage response (37,40).

Mre11 endonuclease and Sae2 are also required to process hairpin-capped DNA ends *in vivo* (47,66,67). However, *in vitro* studies indicate that MRX/N is able to cleave DNA hairpins with no or short (<8 nt) spacers in the absence of Sae2/CtIP (5,68). If the ssDNA spacer between the inverted repeats is large enough to accommodate RPA binding, then MRX cleavage at the ssDNA/dsDNA transition is strongly stimulated by RPA and Sae2 (7). We used an assay in which 300 bp inverted Alu elements, separated by a 12 bp spacer, integrated in the *lys2* gene stimulate ectopic recombination with a truncated *lys2* allele to generate Lys^+ recombinants (47). In this assay, the *sae2-S267A, sae2-2A* and *sae2-5A* mutants exhibit similar (>40-fold) decreases in the formation of recombinants relative to the WT strain. The disparity between the sporulation and inverted-repeat processing results for the *sae2-2A* and *sae2-5A* mutants suggests that Sae2 might function differently at protein-blocked and hairpin-capped ends (Supplementary Figure S5). Consistent with this idea, Kim et al. (28) previously described a *sae2* allele (*sae2-E24V*) with reduced processing of hairpin-capped ends, but that is proficient for sporulation and the purified protein shows normal stimulation of Mre11 endonuclease at protein-blocked ends *in vitro* (5). Our current view of meiotic DSB processing is for MRX-Sae2 to nick 5′ terminated strands ∼270 nt from the Spo11-bound ends, generating an entry site for bi-directional resection by Mre11 3′-5′ exonuclease and Exo1 5′-3′ exonuclease (5,11). Only the MRX-Sae2 catalyzed step is required for meiotic progression and production of viable spores (69). The *in vivo* substrate for MRX-Sae2 processing of Alu inverted repeats is less well characterized. Current models posit that MRX/Sae2 cleave the tip of a hairpin formed on the lagging strand during replication or the hairpin-capped ends formed following Holliday junction endonuclease cleavage at the base of an extruded cruciform (47,58). By both scenarios, the opened hairpin-capped end would require further resection to remove the paired Alu sequences, which lack homology to the ectopic *lys2* donor (Supplementary Figure S5). The deficiency in generating Lys^+ recombinants observed for the *sae2-S267A, sae2-2A* and *sae2-5A* mutants could be at hairpin cleavage or subsequent processing of the opened ends. The roles of Exo1 and Dna2-Sgs1 have not been determined in the inverted Alu recombination assay and this analysis might provide more insight into the mechanisms used to generate Lys^+ recombinants.

SUPPLEMENTARY DATA

Supplementary Data are available at NAR Online.

ACKNOWLEDGEMENTS

We thank M.P. Longhese and H. Zhou for yeast strains and plasmids, M. Foiani for anti-Rad53 antibodies and members of the Symington lab for review of the manuscript and helpful discussions.

FUNDING

National Institutes of Health [CA174653, GM126997].
Conflict of interest statement. None declared.

REFERENCES

1. Chiruvella,K.K., Liang,Z. and Wilson,T.E. (2013) Repair of double-strand breaks by end joining. *Cold Spring Harb. Perspect. Biol.*, **5**, a012757.
2. Symington,L.S., Rothstein,R. and Lisby,M. (2014) Mechanisms and regulation of mitotic recombination in Saccharomyces cerevisiae. *Genetics*, **198**, 795–835.
3. Ira,G., Pellicioli,A., Balijja,A., Wang,X., Fiorani,S., Carotenuto,W., Liberi,G., Bressan,D., Wan,L., Hollingsworth,N.M. *et al.* (2004) DNA end resection, homologous recombination and DNA damage checkpoint activation require CDK1. *Nature*, **431**, 1011–1017.
4. Hustedt,N. and Durocher,D. (2016) The control of DNA repair by the cell cycle. *Nat. Cell Biol.*, **19**, 1–9.
5. Cannavo,E. and Cejka,P. (2014) Sae2 promotes dsDNA endonuclease activity within Mre11-Rad50-Xrs2 to resect DNA breaks. *Nature*, **514**, 122–125.
6. Reginato,G., Cannavo,E. and Cejka,P. (2017) Physiological protein blocks direct the Mre11-Rad50-Xrs2 and Sae2 nuclease complex to initiate DNA end resection. *Genes Dev.*, **31**, 2325–2330.
7. Wang,W., Daley,J.M., Kwon,Y., Krasner,D.S. and Sung,P. (2017) Plasticity of the Mre11-Rad50-Xrs2-Sae2 nuclease ensemble in the processing of DNA-bound obstacles. *Genes Dev.*, **31**, 2331–2336.
8. Anand,R., Ranjha,L., Cannavo,E. and Cejka,P. (2016) Phosphorylated CtIP Functions as a Co-factor of the MRE11-RAD50-NBS1 Endonuclease in DNA End Resection. *Mol. Cell*, **64**, 940–950.
9. Huertas,P., Cortes-Ledesma,F., Sartori,A.A., Aguilera,A. and Jackson,S.P. (2008) CDK targets Sae2 to control DNA-end resection and homologous recombination. *Nature*, **455**, 689–692.
10. Huertas,P. and Jackson,S.P. (2009) Human CtIP mediates cell cycle control of DNA end resection and double strand break repair. *J. Biol. Chem.*, **284**, 9558–9565.

11. Garcia,V., Phelps,S.E., Gray,S. and Neale,M.J. (2011) Bidirectional resection of DNA double-strand breaks by Mre11 and Exo1. *Nature*, **479**, 241–244.
12. Zhu,Z., Chung,W.H., Shim,E.Y., Lee,S.E. and Ira,G. (2008) Sgs1 helicase and two nucleases Dna2 and Exo1 resect DNA double-strand break ends. *Cell*, **134**, 981–994.
13. Gravel,S., Chapman,J.R., Magill,C. and Jackson,S.P. (2008) DNA helicases Sgs1 and BLM promote DNA double-strand break resection. *Genes Dev.*, **22**, 2767–2772.
14. Mimitou,E.P. and Symington,L.S. (2008) Sae2, Exo1 and Sgs1 collaborate in DNA double-strand break processing. *Nature*, **455**, 770–774.
15. Cejka,P., Cannavo,E., Polaczek,P., Masuda-Sasa,T., Pokharel,S., Campbell,J.L. and Kowalczykowski,S.C. (2010) DNA end resection by Dna2-Sgs1-RPA and its stimulation by Top3-Rmi1 and Mre11-Rad50-Xrs2. *Nature*, **467**, 112–116.
16. Niu,H., Chung,W.H., Zhu,Z., Kwon,Y., Zhao,W., Chi,P., Prakash,R., Seong,C., Liu,D., Lu,L. *et al.* (2010) Mechanism of the ATP-dependent DNA end-resection machinery from Saccharomyces cerevisiae. *Nature*, **467**, 108–111.
17. Chen,X., Niu,H., Chung,W.H., Zhu,Z., Papusha,A., Shim,E.Y., Lee,S.E., Sung,P. and Ira,G. (2011) Cell cycle regulation of DNA double-strand break end resection by Cdk1-dependent Dna2 phosphorylation. *Nat. Struct. Mol. Biol.*, **18**, 1015–1019.
18. Symington,L.S. (2016) Mechanism and regulation of DNA end resection in eukaryotes. *Crit. Rev. Biochem. Mol. Biol.*, **51**, 195–212.
19. Mimitou,E.P. and Symington,L.S. (2010) Ku prevents Exo1 and Sgs1-dependent resection of DNA ends in the absence of a functional MRX complex or Sae2. *EMBO J.*, **29**, 3358–3369.
20. Shim,E.Y., Chung,W.H., Nicolette,M.L., Zhang,Y., Davis,M., Zhu,Z., Paull,T.T., Ira,G. and Lee,S.E. (2010) Saccharomyces cerevisiae Mre11/Rad50/Xrs2 and Ku proteins regulate association of Exo1 and Dna2 with DNA breaks. *EMBO J.*, **29**, 3370–3380.
21. Budd,M.E. and Campbell,J.L. (2009) Interplay of Mre11 nuclease with Dna2 plus Sgs1 in Rad51-dependent recombinational repair. *PLoS One*, **4**, e4267.
22. Foster,S.S., Balestrini,A. and Petrini,J.H. (2011) Functional interplay of the Mre11 nuclease and Ku in the response to replication-associated DNA damage. *Mol. Cell Biol.*, **31**, 4379–4389.
23. Limbo,O., Chahwan,C., Yamada,Y., de Bruin,R.A., Wittenberg,C. and Russell,P. (2007) Ctp1 is a cell-cycle-regulated protein that functions with Mre11 complex to control double-strand break repair by homologous recombination. *Mol. Cell*, **28**, 134–146.
24. Langerak,P., Mejia-Ramirez,E., Limbo,O. and Russell,P. (2011) Release of Ku and MRN from DNA ends by Mre11 nuclease activity and Ctp1 is required for homologous recombination repair of double-strand breaks. *PLoS Genet.*, **7**, e1002271.
25. Clerici,M., Mantiero,D., Lucchini,G. and Longhese,M.P. (2006) The Saccharomyces cerevisiae Sae2 protein negatively regulates DNA damage checkpoint signalling. *EMBO Rep.*, **7**, 212–218.
26. Yu,T.Y., Kimble,M.T. and Symington,L.S. (2018) Sae2 antagonizes Rad9 accumulation at DNA double-strand breaks to attenuate checkpoint signaling and facilitate end resection. *Proc. Natl. Acad. Sci. U.S.A.*, **115**, E11961–E11969.
27. Finn,K., Lowndes,N.F. and Grenon,M. (2012) Eukaryotic DNA damage checkpoint activation in response to double-strand breaks. *Cell Mol. Life Sci.*, **69**, 1447–1473.
28. Kim,H.S., Vijayakumar,S., Reger,M., Harrison,J.C., Haber,J.E., Weil,C. and Petrini,J.H. (2008) Functional interactions between Sae2 and the Mre11 complex. *Genetics*, **178**, 711–723.
29. Usui,T., Ogawa,H. and Petrini,J.H. (2001) A DNA damage response pathway controlled by Tel1 and the Mre11 complex. *Mol. Cell*, **7**, 1255–1266.
30. Bonetti,D., Villa,M., Gobbini,E., Cassani,C., Tedeschi,G. and Longhese,M.P. (2015) Escape of Sgs1 from Rad9 inhibition reduces the requirement for Sae2 and functional MRX in DNA end resection. *EMBO Rep.*, **16**, 351–361.
31. Gobbini,E., Villa,M., Gnugnoli,M., Menin,L., Clerici,M. and Longhese,M.P. (2015) Sae2 Function at DNA Double-Strand Breaks Is Bypassed by Dampening Tel1 or Rad53 Activity. *PLoS Genet.*, **11**, e1005685.
32. Ferrari,M., Dibitetto,D., De Gregorio,G., Eapen,V.V., Rawal,C.C., Lazzaro,F., Tsabar,M., Marini,F., Haber,J.E. and Pellicioli,A. (2015) Functional interplay between the 53BP1-Ortholog Rad9 and the Mre11 complex regulates resection, end-Tethering and repair of a Double-Strand break. *PLoS Genet.*, **11**, e1004928.
33. Morin,I., Ngo,H.P., Greenall,A., Zubko,M.K., Morrice,N. and Lydall,D. (2008) Checkpoint-dependent phosphorylation of Exo1 modulates the DNA damage response. *EMBO J.*, **27**, 2400–2410.
34. Ngo,G.H., Balakrishnan,L., Dubarry,M., Campbell,J.L. and Lydall,D. (2014) The 9-1-1 checkpoint clamp stimulates DNA resection by Dna2-Sgs1 and Exo1. *Nucleic Acids Res.*, **42**, 10516–10528.
35. Ngo,G.H. and Lydall,D. (2015) The 9-1-1 checkpoint clamp coordinates resection at DNA double strand breaks. *Nucleic Acids Res.*, **43**, 5017–5032.
36. Baroni,E., Viscardi,V., Cartagena-Lirola,H., Lucchini,G. and Longhese,M.P. (2004) The functions of budding yeast Sae2 in the DNA damage response require Mec1- and Tel1-dependent phosphorylation. *Mol. Cell Biol.*, **24**, 4151–4165.
37. Fu,Q., Chow,J., Bernstein,K.A., Makharashvili,N., Arora,S., Lee,C.F., Person,M.D., Rothstein,R. and Paull,T.T. (2014) Phosphorylation-regulated transitions in an oligomeric state control the activity of the Sae2 DNA repair enzyme. *Mol. Cell Biol.*, **34**, 778–793.
38. Wang,H., Shi,L.Z., Wong,C.C., Han,X., Hwang,P.Y., Truong,L.N., Zhu,Q., Shao,Z., Chen,D.J., Berns,M.W. *et al.* (2013) The interaction of CtIP and Nbs1 connects CDK and ATM to regulate HR-mediated double-strand break repair. *PLoS Genet.*, **9**, e1003277.
39. Cartagena-Lirola,H., Guerini,I., Viscardi,V., Lucchini,G. and Longhese,M.P. (2006) Budding Yeast Sae2 is an In Vivo Target of the Mec1 and Tel1 Checkpoint Kinases During Meiosis. *Cell Cycle*, **5**, 1549–1559.
40. Cannavo,E., Johnson,D., Andres,S.N., Kissling,V.M., Reinert,J.K., Garcia,V., Erie,D.A., Hess,D., Thoma,N.H., Enchev,R.I. *et al.* (2018) Regulatory control of DNA end resection by Sae2 phosphorylation. *Nat. Commun.*, **9**, 4016.
41. Peterson,S.E., Li,Y., Wu-Baer,F., Chait,B.T., Baer,R., Yan,H., Gottesman,M.E. and Gautier,J. (2013) Activation of DSB processing requires phosphorylation of CtIP by ATR. *Mol. Cell*, **49**, 657–667.
42. Liu,X., Wang,X.S., Lee,B.J., Wu-Baer,F.K., Lin,X., Shao,Z., Estes,V.M., Gautier,J., Baer,R. and Zha,S. (2019) CtIP is essential for early B cell proliferation and development in mice. *J. Exp. Med.*, **216**, 1648–1663.
43. Liang,J., Suhandynata,R.T. and Zhou,H. (2015) Phosphorylation of Sae2 mediates forkhead-associated (FHA) domain-specific interaction and regulates its DNA repair function. *J. Biol. Chem.*, **290**, 10751–10763.
44. Williams,R.S., Dodson,G.E., Limbo,O., Yamada,Y., Williams,J.S., Guenther,G., Classen,S., Glover,J.N., Iwasaki,H., Russell,P. *et al.* (2009) Nbs1 flexibly tethers Ctp1 and Mre11-Rad50 to coordinate DNA double-strand break processing and repair. *Cell*, **139**, 87–99.
45. Oh,J., Al-Zain,A., Cannavo,E., Cejka,P. and Symington,L.S. (2016) Xrs2 dependent and independent functions of the Mre11-Rad50 complex. *Mol. Cell*, **64**, 405–415.
46. Amberg,D.C., Burke,D. J. and Strathern,J. N. (2005) *Methods in Yeast Genetics: A Cold Spring Harbor Laboratory Course Manual*. Cold spring Harbor Laboratory Press.
47. Lobachev,K.S., Gordenin,D.A. and Resnick,M.A. (2002) The Mre11 complex is required for repair of hairpin-capped double-strand breaks and prevention of chromosome rearrangements. *Cell*, **108**, 183–193.
48. Krogh,B.O., Llorente,B., Lam,A. and Symington,L.S. (2005) Mutations in Mre11 phosphoesterase motif I that impair Saccharomyces cerevisiae Mre11-Rad50-Xrs2 complex stability in addition to nuclease activity. *Genetics*, **171**, 1561–1570.
49. Donnianni,R.A., Ferrari,M., Lazzaro,F., Clerici,M., Tamilselvan Nachimuthu,B., Plevani,P., Muzi-Falconi,M. and Pellicioli,A. (2010) Elevated levels of the polo kinase Cdc5 override the Mec1/ATR checkpoint in budding yeast by acting at different steps of the signaling pathway. *PLoS Genet.*, **6**, e1000763.
50. Chen,H., Donnianni,R.A., Handa,N., Deng,S.K., Oh,J., Timashev,L.A., Kowalczykowski,S.C. and Symington,L.S. (2015) Sae2 promotes DNA damage resistance by removing the Mre11-Rad50-Xrs2 complex from DNA and attenuating Rad53 signaling. *Proc. Natl. Acad. Sci. U.S.A.*, **112**, E1880–1887.
51. Moreau,S., Ferguson,J.R. and Symington,L.S. (1999) The nuclease activity of Mre11 is required for meiosis but not for mating type

switching, end joining, or telomere maintenance. *Mol. Cell Biol.*, **19**, 556–566.
52. Hopfner,K.P., Karcher,A., Craig,L., Woo,T.T., Carney,J.P. and Tainer,J.A. (2001) Structural biochemistry and interaction architecture of the DNA double-strand break repair Mre11 nuclease and Rad50-ATPase. *Cell*, **105**, 473–485.
53. Gobbini,E., Cassani,C., Vertemara,J., Wang,W., Mambretti,F., Casari,E., Sung,P., Tisi,R., Zampella,G. and Longhese,M.P. (2018) The MRX complex regulates Exo1 resection activity by altering DNA end structure. *EMBO J.*, **37**, e98588.
54. Lam,I. and Keeney,S. (2014) Mechanism and regulation of meiotic recombination initiation. *Cold Spring Harb. Perspect. Biol.*, **7**, a016634.
55. Neale,M.J., Pan,J. and Keeney,S. (2005) Endonucleolytic processing of covalent protein-linked DNA double-strand breaks. *Nature*, **436**, 1053–1057.
56. Manfrini,N., Guerini,I., Citterio,A., Lucchini,G. and Longhese,M.P. (2010) Processing of meiotic DNA double strand breaks requires cyclin-dependent kinase and multiple nucleases. *J. Biol. Chem.*, **285**, 11628–11637.
57. Mimitou,E.P. and Symington,L.S. (2009) DNA end resection: many nucleases make light work. *DNA Repair (Amst.)*, **8**, 983–995.
58. Eykelenboom,J.K., Blackwood,J.K., Okely,E. and Leach,D.R. (2008) SbcCD causes a double-strand break at a DNA palindrome in the Escherichia coli chromosome. *Mol. Cell*, **29**, 644–651.
59. Clerici,M., Mantiero,D., Lucchini,G. and Longhese,M.P. (2005) The Saccharomyces cerevisiae Sae2 protein promotes resection and bridging of double strand break ends. *J. Biol. Chem.*, **280**, 38631–38638.
60. Dibitetto,D., Ferrari,M., Rawal,C.C., Balint,A., Kim,T., Zhang,Z., Smolka,M.B., Brown,G.W., Marini,F. and Pellicioli,A. (2016) Slx4 and Rtt107 control checkpoint signalling and DNA resection at double-strand breaks. *Nucleic Acids Res.*, **44**, 669–682.
61. Lloyd,J., Chapman,J.R., Clapperton,J.A., Haire,L.F., Hartsuiker,E., Li,J., Carr,A.M., Jackson,S.P. and Smerdon,S.J. (2009) A supramodular FHA/BRCT-repeat architecture mediates Nbs1 adaptor function in response to DNA damage. *Cell*, **139**, 100–111.
62. Anand,R., Jasrotia,A., Bundschuh,D., Howard,S.M., Ranjha,L., Stucki,M. and Cejka,P. (2019) NBS1 promotes the endonuclease activity of the MRE11-RAD50 complex by sensing CtIP phosphorylation. *EMBO J.*, **38**, e101005.
63. Durocher,D., Taylor,I.A., Sarbassova,D., Haire,L.F., Westcott,S.L., Jackson,S.P., Smerdon,S.J. and Yaffe,M.B. (2000) The molecular basis of FHA domain:phosphopeptide binding specificity and implications for phospho-dependent signaling mechanisms. *Mol. Cell*, **6**, 1169–1182.
64. Matsuzaki,K., Shinohara,A. and Shinohara,M. (2008) Forkhead-associated domain of yeast Xrs2, a homolog of human Nbs1, promotes nonhomologous end joining through interaction with a ligase IV partner protein, Lif1. *Genetics*, **179**, 213–225.
65. Palmbos,P.L., Wu,D., Daley,J.M. and Wilson,T.E. (2008) Recruitment of Saccharomyces cerevisiae Dnl4-Lif1 complex to a double-strand break requires interactions with Yku80 and the Xrs2 FHA domain. *Genetics*, **180**, 1809–1819.
66. Deng,S.K., Yin,Y., Petes,T.D. and Symington,L.S. (2015) Mre11-Sae2 and RPA collaborate to prevent palindromic gene amplification. *Mol. Cell*, **60**, 500–508.
67. Chen,H., Lisby,M. and Symington,L. (2013) RPA coordinates DNA end resection and prevents formation of DNA hairpins. *Mol Cell*, **50**, 589–600.
68. Paull,T.T. and Gellert,M. (1999) Nbs1 potentiates ATP-driven DNA unwinding and endonuclease cleavage by the Mre11/Rad50 complex. *Genes Dev*, **13**, 1276–1288.
69. Zakharyevich,K., Ma,Y., Tang,S., Hwang,P.Y., Boiteux,S. and Hunter,N. (2010) Temporally and biochemically distinct activities of Exo1 during meiosis: double-strand break resection and resolution of double Holliday junctions. *Mol Cell*, **40**, 1001–1015.